

One- and Two-Dimensional Nuclear Magnetic Resonance Studies on the Compositional Sequence and the Microstructure of Acrylonitrile–Pentyl Methacrylate Copolymers

A. S. BRAR, KAUSHIK DUTTA

Department of Chemistry, Indian Institute of Technology, Hauz Khas, New Delhi 110 016 India

Received 15 September 1997; accepted 24 January 1998

ABSTRACT: The chemical microstructure of acrylonitrile–pentyl methacrylate (A–P) copolymers prepared by photopolymerization using uranyl ion as the photo sensitizer is analyzed by $^{13}\text{C}\{^1\text{H}\}$ nuclear magnetic resonance spectroscopy. The composition of the copolymers were determined by elemental analysis, and comonomer reactivity ratios were determined by the Kelen–Tudos (KT) and the error in variable (EVM) methods. The terminal model reactivity ratios obtained from the EVM method are $r_A = 0.20$ and $r_P = 2.62$. The complete spectral assignment of the overlapping proton and carbon spectra of these copolymers were done with the help of distortionless enhancement by polarization transfer and two-dimensional ^1H – ^{13}C heteronuclear shift correlation (inverse HETCOR) spectroscopy. The assignment of the various conformational and configurational sequences in the proton spectrum were made possible by two-dimensional correlated spectroscopy and total correlation spectroscopy experiments. Monte Carlo simulation was used to study the effect of the degree of polymerization on the triad fractions. © 1998 John Wiley & Sons, Inc. *J Appl Polym Sci* 69: 2507–2516, 1998

INTRODUCTION

The determination of the microstructure in copolymers is of value in establishing structure–properties relationships.¹ Information concerning the microstructure of the polymer is essential for clarifying the polymerization mechanism.^{2–3} The contribution of the two-dimensional (2-D) nuclear magnetic resonance (NMR) spectroscopy (2-D NMR) to the study of homo-^{4–7} and copolymer^{8–9} microstructure has been recognized. DEPT is used extensively for the analysis of the overlapping carbon resonances in the ^{13}C NMR spectra^{10,11} thus helps in compositional and configurational assignments. ^1H – ^{13}C inverse HETCOR is being used frequently for compositional and

configurational^{12,13} assignments of the polymers. A 2-D TOCSY experiment was used to study the spin relay coupling through the magnetization transfer in the copolymer systems.¹⁴ Kapur and Brar have reported the microstructure of acrylonitrile–alkyl methacrylates^{15–17} (alkyl = methyl, ethyl, and butyl) by NMR spectroscopy and did not report the 2-D NMR of these copolymers. To the best of our knowledge, the microstructure of acrylonitrile–pentyl methacrylate (A–P) copolymers has not been reported so far.

In this article, the copolymerization mechanism of A–P copolymers prepared by photo polymerization at room temperature using the uranyl ion as the photo sensitizer was investigated. The ^{13}C NMR spectrum of the A–P copolymers were assigned with the help of DEPT experiment. The methine and the methylene carbon resonances of the acrylonitrile–pentyl methacrylate copolymers are sensitive to compositional and configurational

Correspondence to: A. S. Brar.

sequences. The various compositional sequences were assigned to pentad and hexad sequences with the help of the inverse HETCOR experiments. The methine–methylene protons coupling cross peaks in the 2-D COSY and TOCSY (low mixing time) spectrum were assigned to pentad sequences with the help of the inverse HETCOR experiments. The reactivity ratios of the comonomers were calculated using the Kelen–Tudos¹⁸ (KT) and nonlinear error in variable¹⁹ (EVM) methods using the compositional data obtained from the percentage of nitrogen analysis. The Monte Carlo (MC) simulation method²⁰ was used to study the effect of triad fraction as a function of the degree of polymerization.

EXPERIMENTAL

Pentyl methacrylate was prepared by esterification of methacrylic acid with pentyl alcohol. Pentyl methacrylate was vacuum-distilled and stored below 5°C. The purity of the monomer was checked by high-pressure liquid chromatography (HPLC). Acrylonitrile was distilled under reduced pressure and was stored below 5°C. Uranyl nitrate was mixed with the monomer at different molar feed ratios, and polymerization was carried out at room temperature.³ The percentage of conversion was kept below 10% by precipitating the copolymers in methanol. The copolymers were purified by dissolving and reprecipitating in the chloroform–methanol system.

The copolymer composition was calculated from the percentage of nitrogen of the copolymers. The C, H, and N analysis were done on Perkin–Elmer 240C elemental analyzer instrument. The molecular weight of the copolymers were determined by gel permeation chromatography (GPC) using narrow polystyrene standards in tetrahydrofuran (THF).

NMR experiments were performed in CDCl₃ on Bruker DPX-300 spectrometer at a frequency of 300.13 and 75.5 MHz for ¹H and ¹³C{¹H} NMR spectra, respectively. Distortionless enhancement by polarization transfer (DEPT) measurements were carried in CDCl₃ using the standard pulse sequence with a *J* modulation time of 3.7 ms (*J*_{CH} = 135 Hz) with 2-s delay time. A two-dimensional proton detected ¹H–¹³C heteronuclear chemical shift correlation was recorded in CDCl₃ using the standard pulse sequence.²¹ A total of 32 scans were accumulated with a relaxation delay of 2 s for each of the 512 *t*₁ experiments. The DQFCOSY

experiment, with 32 scans being collected for each *t*₁ value was carried out in CDCl₃. A total of 512 spectra each containing the 1K data points were accumulated. Two-dimensional homonuclear total correlation spectroscopy (TOCSY) spectrum was recorded at a 4- and 80-ms mixing time. A total of 32 scans were accumulated with a relaxation delay of 2 s for each of the 512 *t*₁ experiments. The details of the Lorentzian shape curve fitting have been described elsewhere.³ All regression converged to $\chi^2 < 1$.

RESULTS AND DISCUSSION

Reactivity Ratio Determination

The copolymer composition of the A–P copolymers were determined from the percentage of nitrogen content of the copolymers. Table I shows the comonomer mole fractions in the feed and in the copolymer, along with the nitrogen content in the copolymers. The initial estimate of the reactivity ratios was done by the KT method. The values of the terminal model reactivity ratios obtained from the KT plot are $r_A = 0.21 \pm 0.02$ and $r_P = 2.65 \pm 0.38$. These values, along with the copolymer composition data, were used to calculate the reactivity ratios using the EVM program. The percentage of error in measuring the comonomer composition in the feed and in the copolymer were taken for the EVM program as 1 and 3%, respectively. The values of the reactivity ratios obtained from EVM are $r_A = 0.20$ and $r_P = 2.62$. A 95% joint confidence interval plot for the acrylonitrile–pentyl methacrylate comonomer pair is shown in Figure 1. The copolymer composition obtained from the copolymer equation using the terminal model reactivity ratios ($r_A = .20$ and $r_P = 2.62$) are compared with those found experimentally and are shown in Table I. The experimental points are in good agreement with the theoretically calculated ones, indicating that the reactivity ratios obtained from the compositional data are more reliable. The number-average (M_n) and weight-average (M_w) molecular weights and polydispersity of the A–P copolymers are given in Table I.

¹³C AND ¹H NUCLEAR MAGNETIC RESONANCE STUDIES

The ¹³C{¹H} NMR spectrum of the A–P copolymer ($F_A = 0.47$) in CDCl₃ is shown in Figure 2. The

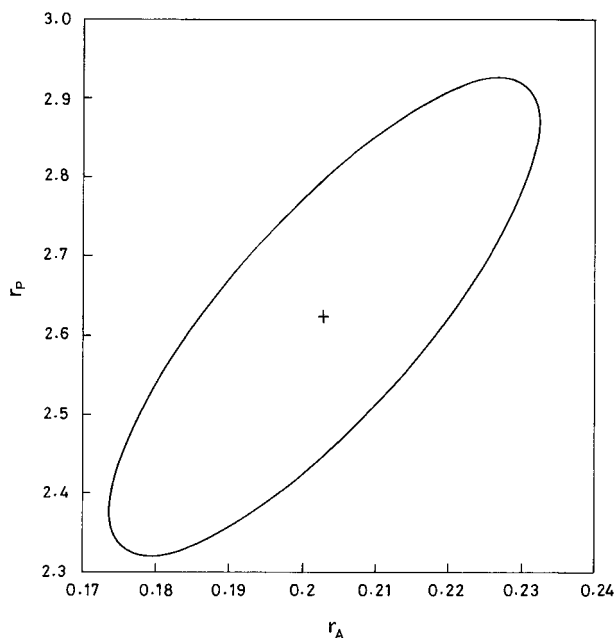
Table I The Feed Mole Fractions, Percent Nitrogen, Percent Conversion, Copolymer Compositions Determined Experimentally and Calculated Theoretically and Molecular Weight Averages for Acrylonitrile–Pentyl Methacrylate Copolymers

No.	Feed Mole Fraction (f_A)	Percent Nitrogen	Percent Conversion	Copolymer Composition (F_A)		$M_n^b \times 10^{-4}$	$M_w^b \times 10^{-4}$	PD ^b
				Expt.	Theor. ^a			
1	0.95	15.9	4.5	0.82	0.81	—	—	—
2	0.90	10.9	3.6	0.67	0.68	—	—	—
3	0.85	9.0	6.2	0.60	0.59	3.7	9.8	2.6
4	0.80	7.0	5.5	0.52	0.52	2.7	6.3	2.3
5	0.75	6.1	4.8	0.47	0.46	2.9	6.9	2.4
6	0.70	5.1	6.0	0.41	0.41	2.8	8.6	3.1
7	0.60	3.6	4.3	0.32	0.32	3.9	10.7	2.7
8	0.50	1.8	6.9	0.18	0.25	2.7	5.8	2.1

^a From the copolymer equation.

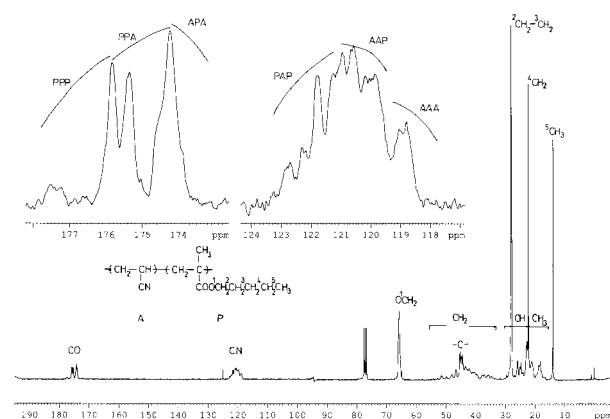
^b M_n is the number average, M_w is the weight average, and PD is the polydispersity.

multiplets around $\delta 178.0$ – 173.0 and $\delta 124.0$ – 118.0 ppm are assigned to carbonyl and nitrile carbon resonances. The spectral region $\delta 10.0$ – 70.0 ppm is very complex and overlapping. This can be assigned to aliphatic carbon in the backbone and the side chain methyl, methylene, and $-\text{OCH}_2$ carbons. On comparison with the homopolymer spectra, it is clear that there is a considerable amount of overlap of the quaternary carbon ($\delta 44.0$ – 45.5 ppm) with the β -methylene car-

**Figure 1** The 95% joint confidence intervals for the acrylonitrile–pentyl methacrylate comonomer pair.

bons. Similarly, there is considerable overlap between the methine, α -methyl, and the alkyl side chain methylene carbons signals. The extent of the overlap of the various carbon signals cannot be ascertained from the $^{13}\text{C}\{^1\text{H}\}$ NMR spectra alone. These overlapping carbon regions can be resolved by employing DEPT and ^1H – ^{13}C inverse HETCOR experiments.

Figure 3 shows the DEPT-135 spectra for 3 different compositions of the A–P copolymers, in which the methyl and methine carbon resonances are positive and the methylene carbon resonances are negative. The methine and the methyl carbon resonances range from $\delta 15.0$ – 30.0 ppm and those for methylene carbon resonance range from $\delta 30.0$ – 60.0 ppm. The methylene carbon reso-

**Figure 2** The $^{13}\text{C}\{^1\text{H}\}$ NMR spectrum of acrylonitrile–pentyl methacrylate (A–P) copolymer ($F_A = 0.47$) in CDCl_3 .

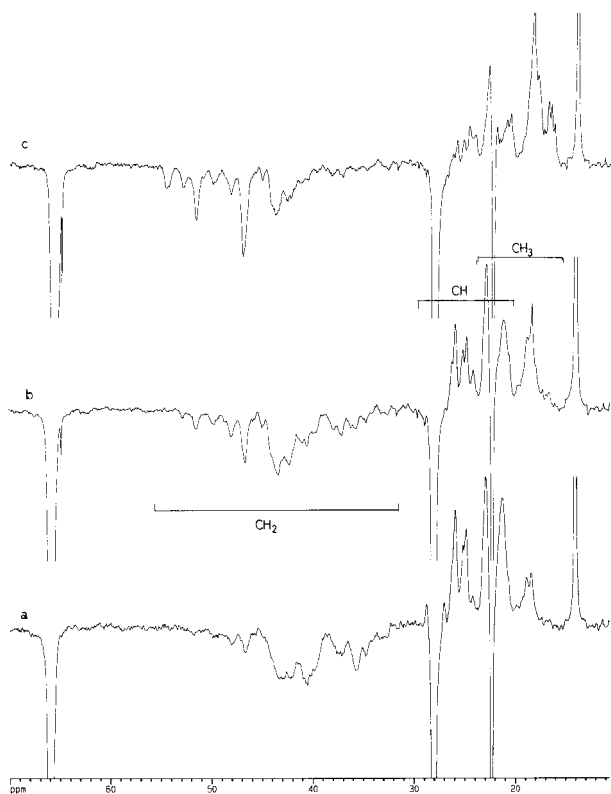


Figure 3 The DEPT-135 spectra of A-P copolymers: (a) $F_A = 0.60$, (b) $F_A = 0.47$, and (c) $F_A = 0.18$, in CDCl_3 .

nances of the alkyl side chain are around $\delta 65.9$ – 65.4 ($-\text{OCH}_2$), 28.11 ($^2\text{CH}_2$), 27.85 ($^3\text{CH}_2$), and 22.30 ($^4\text{CH}_2$) ppm. The methyl carbon signal is seen at $\delta 13.97$ ppm. The $-\text{OCH}_2$ carbon resonances are also sensitive to triad sequences. Figure 4 shows the methine subspectra for series of A-P copolymers of different compositions.

The methine carbon resonance shows both stereochemical and compositional sensitivity. The methine carbon region can be split into 3 broad envelopes. These 3 envelopes vary with the change in the copolymer compositions and can be assigned to AAA ($\delta 26.3$ – 29.5 ppm), AAP (PAA) ($\delta 23.8$ – 26.3 ppm), and PAP ($\delta 21.0$ – 23.8 ppm) triad sequences. These triad fractions further show signals, which can be assigned to configurational or compositional sequences (Table II). In the AAA region, the 3 multiplets at $\delta 28.67$, 27.85 , and 27.02 ppm are assigned to rr, mr (rm), and mm tacticity, respectively, on the basis of the signals observed in the homopolymer spectrum. The corresponding methine proton can be assigned with the help of inverse HETCOR experiments. Figure 5(a) and (b) shows the expanded inverse

HETCOR spectra of the methine region of 2 different compositions.

The AAP triad fraction can be divided into 3 regions, which are assigned to pentad compositional sequences on the basis of change in the intensity with the copolymer composition (Fig. 4). Further splittings within these pentad sequences, which do not change with the copolymer composition, are due to configurational sensitivity. The signals at $\delta 25.92$ and 26.18 ppm are assigned to AAmAPA and AArAPA, respectively. The methine carbon of AAmAPA pentad shows 2 cross peaks at $\delta 25.92/2.85$ and $\delta 25.92/2.62$ ppm in the proton axis in Figure 5(a). This may be due to the different configurational arrangement (AAMArPA and AAmAmPA) of the -P unit attached to the AmAP central triad. However, the methine proton of the AArAPA pentad shows only 1 cross peak at $\delta 26.18/2.82$ ppm, which suggests that the methine proton of the ArAP central triad is probably insensitive to the configurational arrangement of the adjacent -P unit. The signals at $\delta 25.08$ and $\delta 24.74$ ppm are assigned to AArAPP and

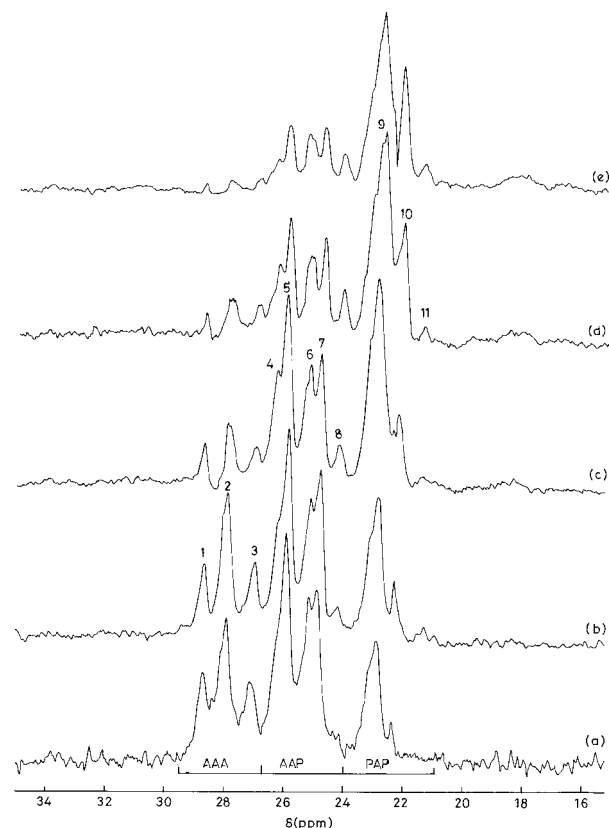


Figure 4 The DEPT-90 spectra showing the methine carbon signals of different copolymer compositions (F_A): (a) 0.67, (b) 0.60, (c) 0.47, (d) 0.32, and (e) 0.18.

Table II Triad Compositions Calculated from NMR Spectra, Monte Carlo Simulations, and the Alfrey–Mayo Model in Acrylonitrile–Pentyl Methacrylate A–P Copolymer

No.	Feed Mole Fraction of A	Triads	Triad Concentration ^a		
			¹³ C{ ¹ H}NMR	Alfrey–Mayo	Monte Carlo
1	0.90	AAA	0.45	0.42	0.55
		AAP	0.44	0.46	0.38
		PAP	0.11	0.13	0.07
		PPP	0.53	0.60	0.74
		PPA	0.40	0.35	0.24
		APA	0.06	0.05	0.02
2	0.85	AAA	0.27	0.29	0.33
		AAP	0.47	0.50	0.49
		PAP	0.26	0.22	0.18
		PPP	0.44	0.47	0.61
		PPA	0.45	0.43	0.34
		APA	0.11	0.10	0.05
3	0.80	AAA	0.21	0.20	0.18
		AAP	0.47	0.49	0.50
		PAP	0.32	0.31	0.32
		PPP	0.38	0.36	0.46
		PPA	0.45	0.48	0.44
		APA	0.17	0.16	0.10
4	0.75	AAA	0.17	0.14	0.10
		AAP	0.47	0.47	0.43
		PAP	0.36	0.39	0.47
		PPP	0.30	0.28	0.34
		PPA	0.53	0.50	0.49
		APA	0.17	0.22	0.17
5	0.70	AAA	0.13	0.10	0.06
		AAP	0.41	0.44	0.37
		PAP	0.46	0.46	0.57
		PPP	0.23	0.22	0.21
		PPA	0.52	0.50	0.49
		APA	0.25	0.28	0.29
6	0.60	AAA	0.09	0.05	0.02
		AAP	0.34	0.36	0.26
		PAP	0.57	0.59	0.72
		PPP	0.13	0.13	0.09
		PPA	0.46	0.46	0.41
		APA	0.41	0.41	0.50
7	0.50	AAA	0.06	0.03	0.01
		AAP	0.26	0.28	0.18
		PAP	0.68	0.69	0.80
		PPP	0.07	0.08	0.04
		PPA	0.41	0.40	0.32
		APA	0.52	0.52	0.64

^a A- and P-centered triad fractions add up to unity.

AAmAPP pentad sequences, respectively. Similarly, AAmAPP pentad shows 2 cross peaks in the proton axis at δ 24.74/2.81 (AAmArPP) and 24.74/2.54 (AAmAmPP) ppm, and AArAPP shows only 1 cross peak at δ 25.08/2.81 ppm, as shown in Figure 5(a). The PAAPP pentad sequence is assigned

at δ 24.08 ppm, and the corresponding methine proton resonances at δ 2.79 ppm [Fig. 5(b)]. In the PAP region, there are 3 clear regions that show variation with composition and thus can be assigned to pentad sequences (Fig. 4). The signals at δ 22.79, 22.14, and 21.35 ppm are assigned to

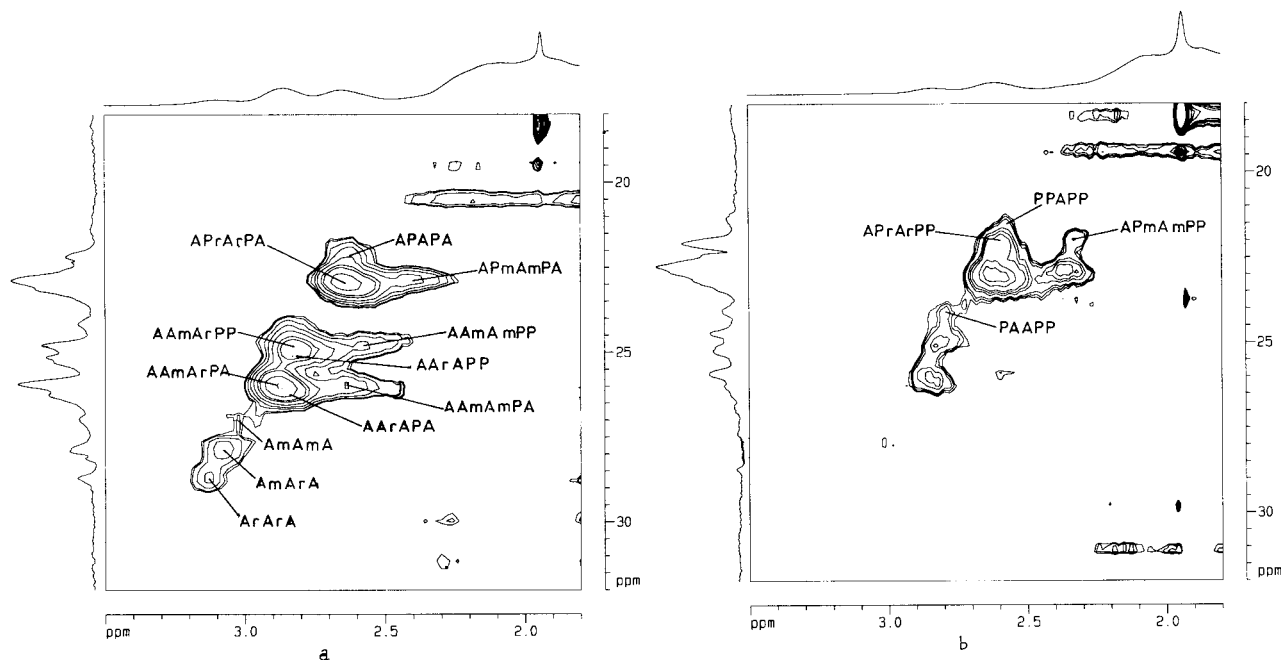


Figure 5 The methine region of the inverse-HETCOR spectrum of A-P copolymers: (a) $F_A = 0.47$ and (b) $F_A = 0.18$ (^1H -x axis and ^{13}C -y axis).

APAPA, APAPP, and PPAPP pentad sequences, respectively. These pentad sequences further show configurational sensitivity, which are assigned in Figure 5(b). Thus, all the different methine protons in the ^1H spectrum have been assigned. All the methine carbon assignments are given in Table III.

Figure 6 shows the methylene carbon region of the A-P copolymers. The methylene carbons can be assigned to the following 3 dyad regions: AA ($\delta 30.0$ – 39.0 ppm), AP (PA) ($\delta 39.0$ – 45.0 ppm),

Table III The Compositional and Configurational Assignments of the Methine Region of A-P Copolymers

Peak No.	Chemical Shift	Assignments
1	28.67	ArArA
2	27.85	ArAmA
3	27.02	AmAmA
4	26.18	AArAPA
5	25.92	AAmAPA
6	25.08	AArAPP
7	24.74	AAmAPP
8	24.08	PAAPP
9	22.79	APAPA
10	22.14	APAPP
11	21.35	PPAPP

and PP ($\delta 45.0$ – 55.0 ppm). The intensities of the lines within each dyad vary with the copolymer composition and thus can be assigned to tetrad sequences. The 3 signals in the AA dyad region are assigned to AAAA ($\delta 32.0$ – 34.5 ppm), AAAP (PAAA) ($\delta 34.0$ – 36.5 ppm), and PAAP ($\delta 36.5$ – 39.0 ppm). The splitting within these tetrads can be assigned to hexad sequences with the help of ^1H - ^{13}C inverse HETCOR spectra [Fig. 7(a) and (b)]. There are 3 cross peaks within these tetrads, which vary in intensity with copolymer composition and can be assigned to hexad sequences. Thus, the cross peaks at $\delta 33.19/2.16$, $\delta 33.40/2.04$, $\delta 34.88/2.14$, $\delta 35.37/1.97$, $\delta 35.93/1.74$, $\delta 36.65/2.10$, $\delta 37.14/1.89$, and $\delta 38.25/1.72$ ppm are assigned to AAAAAP (PAAAAA), PAAAAP, AAAAPA, PAAAPA, PAAAPP, APAAPA, APAAPP, and PPAAPP, respectively.

The AP(PA) dyad can also be divided into the following 3 tetrad: AAPA ($\delta 39.0$ – 41.0 ppm), AAPP + APAP ($\delta 41.0$ – 43.0 ppm), and PAPP ($\delta 43.0$ – 45.0 ppm). The splitting pattern within these tetrads are complex and overlapping, and further assignments are difficult. The 3 PP-centered tetrads, APPA, PAPP(PPPA), and PPPP, can be assigned around $\delta 45.5$ – 47.5 , $\delta 47.5$ – 52.0 , and $\delta 51.0$ – 56.0 ppm, respectively (Fig. 6). The further splitting in the PPPP and PPPA tetrads can be assigned to hexad sequences on the basis

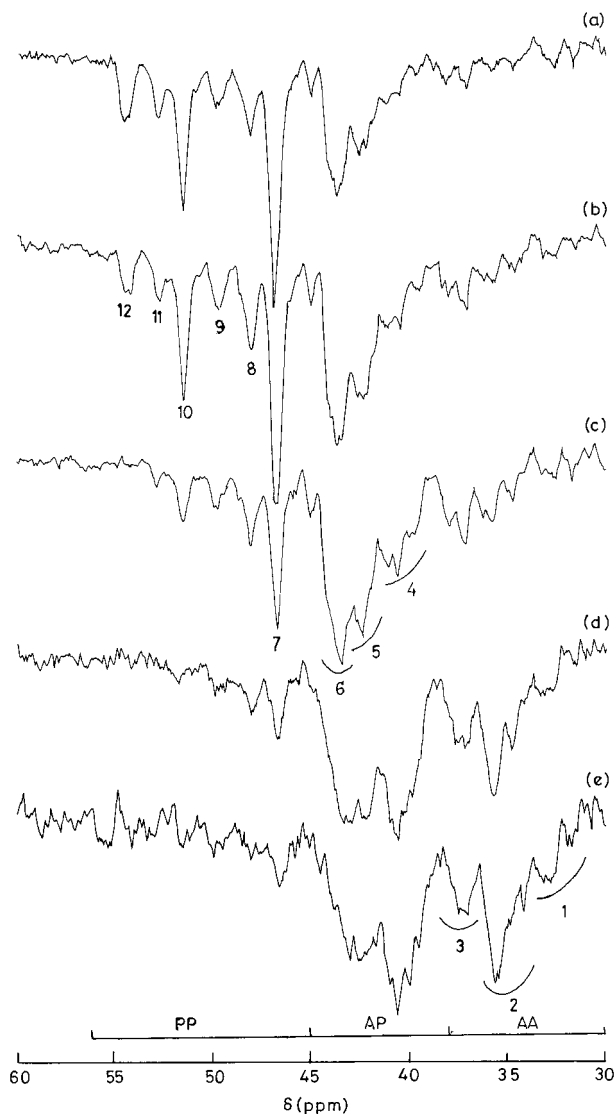


Figure 6 The DEPT-135 spectra showing the methylene carbon signals of different copolymer compositions (F_A): (a) 0.18, (b) 0.32, (c) 0.47, (d) 0.60, and (e) 0.67.

of variation of the peaks with the composition. From the inverse HETCOR spectra [Fig. 7(b)], the cross peaks at $\delta 54.79/1.85$, $53.14/1.95$, $51.99/2.06$, $51.99/1.92$, $50.07/1.99$, and $48.66/2.07$ ppm are assigned to PPPPPP, PPPPPA (APPPPP), APPPPA, PPPPAP, PPPPAA, and APPPAA, respectively. All the methylene carbon assignments are given in Table IV.

The ^1H spectrum of the A-P copolymer (Fig. 8) is very broad and overlapping. The overlapping methylene protons of the side chain can be distinguished from the main chain methylene protons by 2-D ^1H - ^{13}C inverse HETCOR spectroscopy. The methine proton signals are seen around $\delta 3.3$ –

2.1 ppm. All the methine proton signals are assigned to various pentad sequences with the help of inverse HETCOR, as shown earlier. Due to the cancellation of the cross peaks in the DQFCOSY spectrum, these cross peaks are clearly seen in the shorter mixing time TOCSY spectrum. At a shorter mixing time, one can see the direct coupling (AM spin type) between the bonded protons; whereas at a higher mixing time, one can see the relay coupling (AMX spin type) through the magnetization transfer. All the methine-methylene protons coupling cross peaks, which are seen in the low mixing time TOCSY spectrum (4 ms), are all assigned, as shown in the Figure 9.

The nitrile ($-\text{CN}$) and carbonyl ($>\text{C}=\text{O}$) carbon resonances showed multiplets, indicating that they are sensitive towards the compositional sequences and can be used for the assessment of the copolymerization mechanism. The expanded $^{13}\text{C}\{^1\text{H}\}$ NMR spectra of the nitrile and the carbonyl carbon resonances of the A-P copolymer are shown in Figure 2. The signals around $\delta 118.0$ – 119.4 , $\delta 119.0$ – 121.15 , and $\delta 121.1$ – 124.0 ppm are assigned to AAA, AAP (PAA), and PAP, respectively, on the basis of the variation in the spectra with the copolymer composition. The addition of the M unit to the AAA triad causes the downfield shift in the position of AAP and PAP triads due to the deshielding effect of the carbonyl group.

The carbonyl carbon resonance signal also shows triad sensitivity. The resonance signals around $\delta 173.0$ – 174.2 , $\delta 174.0$ – 175.9 , and $\delta 175.5$ – 178.0 ppm are assigned as APA, PPA (APP), and PPP, respectively. These assignments are based on the variation in the spectra with the copolymer composition. The concentration of various A- and P-centered triads were calculated from the relative areas of the resonance signals. Assuming the Alfrey-Mayo (first-order Markov terminal model) to be valid at any moment for these low conversion copolymers, the triad fractions can be calculated using the terminal model reactivity ratios $r_A = 0.20$ and $r_P = 2.62$. Table II shows the A- and P-centered triad fraction calculated from Alfrey-Mayo model using Harwood's program²² and the experimentally determined triad fraction. There is a good agreement between the calculated and the experimentally (NMR) determined triad fractions (correlation coefficient $R = 0.990$).

The conditional probabilities²³ $P_{P/A}$ and $P_{A/P}$ were calculated from the triad concentrations. The value of $P_{A/P}$ decreases linearly from 0.74 to 0.28 with the decrease in acrylonitrile content,

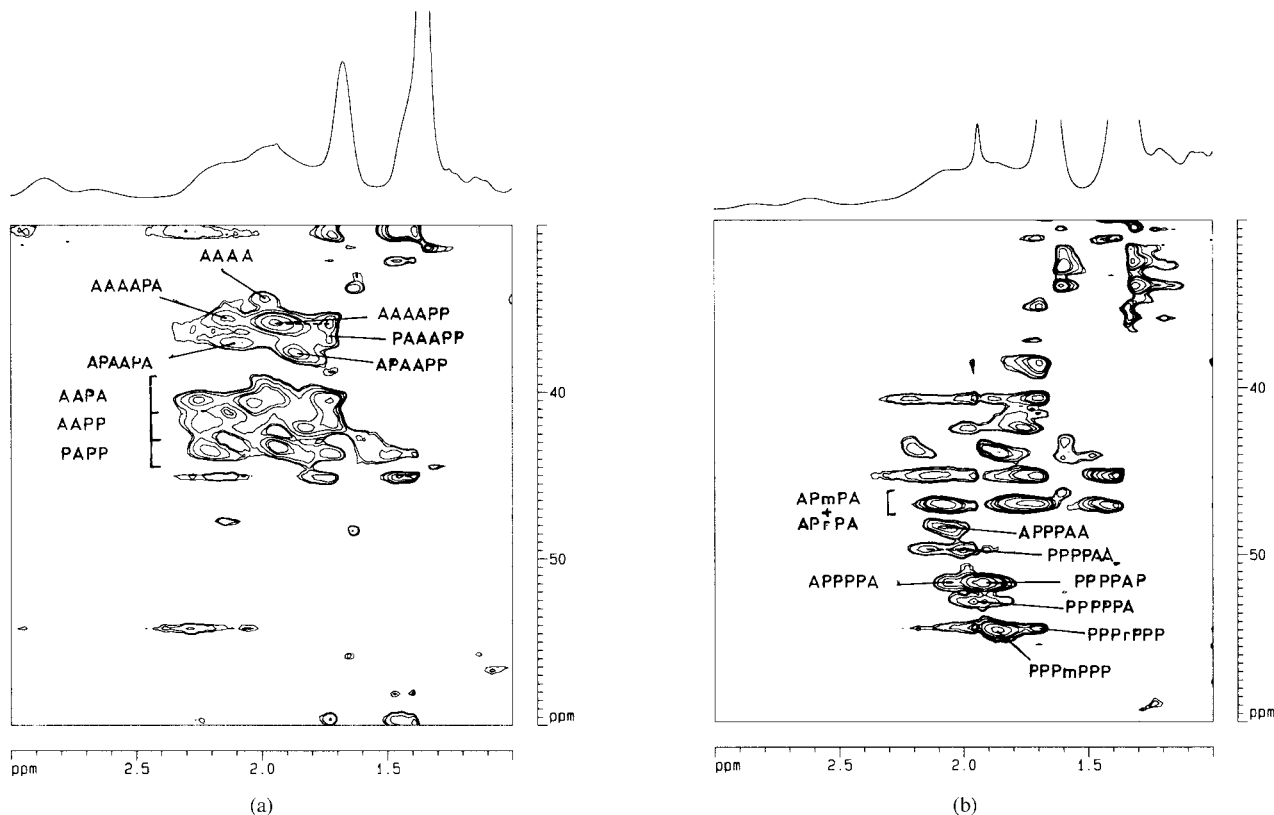


Figure 7 The methylene region of the inverse-HETCOR spectrum of A-P copolymers: (a) $F_A = 0.60$ and (b) $F_A = 0.18$ (^1H -x axis and ^{13}C -y axis).

while the value of $P_{P/A}$ increases linearly from 0.33 to 0.81 as the concentration of A unit increases. The terminal model reactivity ratios were calculated from the slopes of the plots of $[1/P_{P/A} - 1]$ versus f_A/f_P and $[1/P_{A/P} - 1]$ versus f_P/f_A ,

respectively. The values of the terminal model reactivity ratios are $r_A = 0.21$ and $r_P = 2.56$, which are within the experimental error of those calculated from the compositional data.

Table IV The Compositional and Configurational Assignments of the Methylene Region of A-P Copolymers

Peak No.	Chemical Shift in ppm	Assignments
1	32.0–34.5	AAAA
2	34.5–36.5	AAAP (PAAA)
3	36.5–39.0	PAAP
4	39.0–41.0	AAPA
5	41.0–43.0	AAPA + APAP
6	43.0–45.0	PAPP
7	46.99	APmPA + APrPA
8	48.66	APPPAA
9	50.07	PPPPAA
10	51.99	APPPPA + PPPPAP
11	53.14	PPPPPA
12	54.79	PPPPPP

MONTE CARLO SIMULATION STUDIES

The MC simulation method can be used to determine the triad fractions at various degrees of polymerization. The detailed methodology of the MC simulation is given elsewhere.²⁰ Figure 10 shows the variation of the A- and P-centered triad concentration as a function of fractional conversion for different feed mole fractions. The AAA triad fraction is seen to increase as the conversion increases. As the f_A decreases, the triad fraction (AAA) increases only at higher conversion as pentyl methacrylate is consumed faster than acrylonitrile comonomer. The AAP triad fraction concentration first increases, goes through a maximum, and then decreases as the conversion increases. The maximum shifts toward higher conversion as f_A decreases. The PAP triad fraction

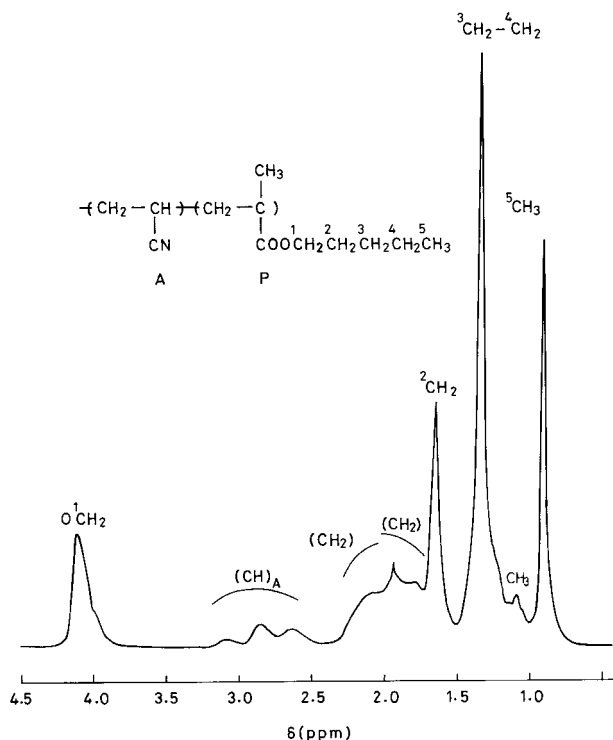


Figure 8 The ^1H NMR spectrum of acrylonitrile-pentyl methacrylate (A-P) copolymer ($F_A = 0.47$) in CDCl_3 .

decreases as the fractional conversion increases. Pentyl methacrylate has higher reactivity ratios, and f_P is higher, so the PAP triad fraction is formed initially, but at higher conversion, it de-

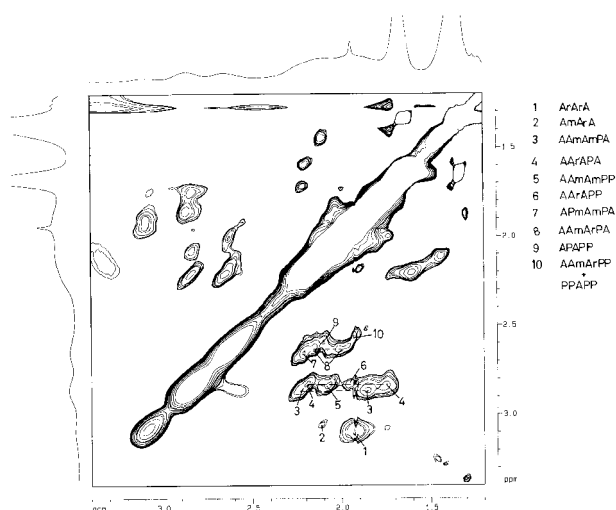


Figure 9 The 2-D-TOCSY spectrum of the acrylonitrile-pentyl methacrylate copolymer ($F_A = 0.47$) in CDCl_3 .

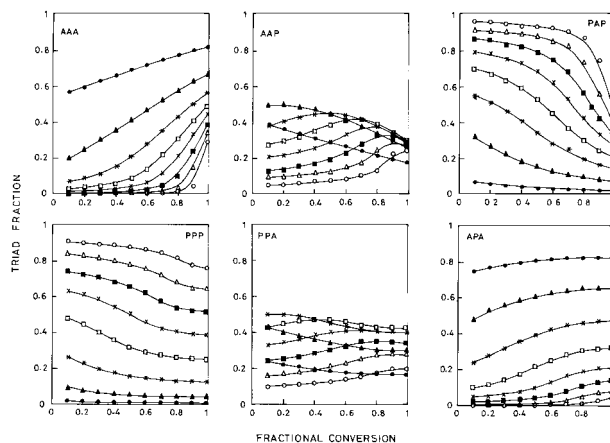


Figure 10 Variation of A- and P-centered triad fractions plotted as a function of fractional conversion for different feed mole fractions: $f_A = 0.90$ (\bullet), $f_A = 0.80$ (\blacktriangle), $f_A = 0.70$ ($*$), $f_A = 0.60$ (\square), $f_A = 0.50$ (\times), $f_A = 0.40$ (\blacksquare), $f_A = 0.30$ (\triangle), and $f_A = 0.20$ (\circ).

creases much sharply as pentyl methacrylate is consumed faster.

The PPP triad concentration decreases as the fractional conversion increases. The PPA triad fraction for the feed mole fraction between $0.80 > f_A > 0.20$ increases, goes through a maximum, and then decreases as the degree of polymerization increases. The APA triad fraction increases as the fractional conversion increases.

CONCLUSIONS

The reactivity ratios of the A-P copolymer system are $r_A = 0.20$ and $r_P = 2.62$. The overlapping and broad signals in the carbon and proton spectra were assigned completely to various compositional and configurational sequences with the help of inverse-HETCOR, COSY, and TOCSY experiments. The methine and the methylene carbon resonances are assigned to the pentad and hexad level, respectively. The copolymerization mechanism of the A-P copolymers were found to follow the first-order Markov model.

The authors thank the Council of Scientific and Industrial Research (CSIR), India, for funding this work. The authors also thank the Department of Chemistry, Indian Institute of Technology, Delhi, for providing the NMR facility.

REFERENCES

1. F. A. Bovey, *High Resolution NMR of Macromolecules*, Academic Press, New York, 1972.

2. J. D. Borbely, D. J. T. Hill, A. P. Lang, and J. H. O'Donnell, *Macromolecules*, **24**, 2208 (1991).
3. A. S. Brar, K. Dutta, and G. S. Kapur, *Macromolecules*, **28**, 8735 (1995).
4. M. Suchopareck and J. Spevacek, *Macromolecules*, **26**, 102 (1993).
5. A. Bulai, M. L. Jimeno, and J. S. Roman, *Macromolecules*, **28**, 7363 (1995).
6. P. J. Hocking and R. H. Marchessault, *Macromolecules*, **28**, 6401 (1995).
7. L. Dong, J. D. J. Hill, J. H. O'Donnell, and A. W. Whittaker, *Macromolecules*, **27**, 1830 (1994).
8. A. S. Brar and M. Malhotra, *Macromolecules*, **29**, 7040 (1996).
9. A. M. Aerdt, J. W. deHann, A. L. German, and G. P. M. vander Velden, *Macromolecules*, **24**, 1473 (1991).
10. P. F. Barron, D. J. T. Hill, J. H. O'Donnell, and P. W. O'Sullivan, *Macromolecules*, **17**, 1967 (1984).
11. J. D. Borbely, D. J. T. Hill, A. P. Lang, and J. H. O'Donnell, *Polym. Int.*, **26**, 171 (1991).
12. A. Bulai, M. L. Jimeno, A. A. de Queiroz, A. Galardo, and J. S. Roman, *Macromolecules*, **29**, 3240 (1996).
13. C. Mijangos and D. Lopez, *Macromolecules*, **28**, 1364 (1995).
14. B. T. Doan, B. Gillet, B. Blondel, and J. C. Beloeil, *Fuel*, **74**, 1806 (1995).
15. G. S. Kapur and A. S. Brar, *Polymer*, **32**, 1112 (1991).
16. G. S. Kapur and A. S. Brar, *J. Polym. Sci., Part A: Polym. Chem.*, **29**, 479 (1991).
17. G. S. Kapur and A. S. Brar, *Makromol. Chem.*, **192**, 2733 (1991).
18. T. Kelen and F. Tudos, *J. Macromol. Sci. Chem.*, **A9**, 1 (1975).
19. M. Dube, R. A. Sanyal, A. Penlidis, K. F. O'Driscoll, and P. M. Reilly, *J. Polym. Sci., Polym. Chem. Ed.*, **29**, 703 (1991).
20. A. S. Brar, B. Jayaram, and K. Dutta, *J. Polym. Mater.*, **10**, 269 (1993).
21. A. Bax and S. Subramanian, *J. Magn. Reson.*, **67**, 565 (1986).
22. H. J. Harwood, *J. Polym. Sci.*, **25**, 37 (1968).
23. J. L. Koenig, *Chemical Microstructure of Polymer Chains*, Wiley-Interscience, New York (1980).